



PERGAMON

Available online at [www.sciencedirect.com](http://www.sciencedirect.com)

SCIENCE @ DIRECT®



[www.actamat-journals.com](http://www.actamat-journals.com)

Scripta Materialia 49 (2003) 87–92

# Cyclic fatigue crack propagation behavior of $Ti_3SiC_2$ synthesized by pulse discharge sintering (PDS) technique

H. Zhang<sup>a,\*</sup>, Z.G. Wang<sup>a</sup>, Q.S. Zang<sup>a</sup>, Z.F. Zhang<sup>b</sup>, Z.M. Sun<sup>b</sup>

<sup>a</sup> *Materials Fatigue and Fracture Division, Shenyang National Laboratory for Materials Science, Institute of Metal Research, Chinese Academy of Sciences, Wenhua road 72, Shenyang 110016, PR China*

<sup>b</sup> *National Institute of Advanced Industrial Science and Technology, 4-2-1, Nigatake, Miyagino-ku, Sendai 983-8551, Japan*

Received 11 January 2003; received in revised form 25 March 2003; accepted 27 March 2003

## Abstract

Cyclic fatigue properties of  $Ti_3SiC_2$  were investigated. When the crack was shorter, it was always arrested due to rapidly increasing crack-tip shielding. Multiple energy dissipative mechanisms including crack deflecting, branching, delamination and grain bridging are responsible for the observed stable crack propagation and high crack growth resistance in this material.

© 2003 Acta Materialia Inc. Published by Elsevier Science Ltd. All rights reserved.

*Keywords:*  $Ti_3SiC_2$ ; Fatigue; Fracture; Microstructure

## 1. Introduction

$Ti_3SiC_2$  is a ternary carbide which has many properties common to ceramic materials, such as high oxidation resistance, refractory and lack of macroscopic plasticity [1]. Besides, it is relatively soft with Vickers hardness as low as about 4 GPa and readily machinable using commonly available cutting-tools [2–4]. In the past decade, many efforts have been devoted to the fabrication of  $Ti_3SiC_2$  with high density and purity. Dense and pure polycrystalline  $Ti_3SiC_2$  has been fabricated by some techniques, e.g. relatively hot-pressing technique from Ti/SiC/graphite powders [1] and pulse

discharge sintering (PDS) technique from Ti/Si/TiC powders [5]. A contact damage study [2] has shown that  $Ti_3SiC_2$  deformed by slipping along basal plane in individual grains and intergranular cracking mode. Fatigue and fracture properties of  $Ti_3SiC_2$  were first studied by Gilbert et al. [6]. Compression tests at low temperature have shown that  $Ti_3SiC_2$  exhibited ductility by a combination of delamination and kink-band formation in individual grains [7,8]. The effect of temperature, strain rate and grain size on the mechanical properties of  $Ti_3SiC_2$  in tension has been characterized [9]. The principal goal of the present study is to study the shielding ability of grain bridging zone in the wake to crack growth rates in different stages of crack growth, specifically at small crack region, and investigate further the cyclic fatigue crack propagation behavior of  $Ti_3SiC_2$  fabricated by PDS technique. The dependence of fatigue

\* Corresponding author. Tel.: +86-2483978270; fax: +86-2423891320.

E-mail address: [h Zhang@imr.ac.cn](mailto:h Zhang@imr.ac.cn) (H. Zhang).

crack growth rates on  $K_{\max}$  and  $\Delta K$  is investigated in order to disclose the salient mechanisms for fatigue crack propagation and fracture.

## 2. Experimental procedure

$\text{Ti}_3\text{SiC}_2$  in the present study was fabricated by PDS technique. The optimized sintering temperature in the range of 1250–1300 °C produced a duplex grain microstructure with both relative density and purity higher than 99% [5]. Such duplex structure consists of both elongated and equiaxed grains. Grains with elongated morphology were embedded in the equiaxed matrix grains, showing a heterogeneous duplex microstructure. The elongated grain was typically  $\sim 50 \mu\text{m}$  long and  $\sim 15 \mu\text{m}$  wide, while the average size of equiaxed grain was  $\sim 5 \mu\text{m}$ . Characteristic microstructures are shown in Fig. 1a. Layered nature of  $\text{Ti}_3\text{SiC}_2$  grains can be clearly seen in Fig. 1b in an elongated grain.

Cyclic fatigue tests were performed on a Shimadzu testing machine with a load capacity of 1 kN. Compact-tension (CT) specimens of 2.6 mm thick, 19.5 mm width were fabricated by means of electrical discharging machining. Specimen surfaces were mechanically polished down to  $\sim 1 \mu\text{m}$  diamond paste. Specimens were cycled at a frequency of 20 Hz (sine wave) under load control at a load ratio  $R$  (ratio of minimum to maximum applied load) of 0.1 and 0.5. All tests were conducted at room temperature ( $\sim 20 \text{ }^\circ\text{C}$ ) and relative humidity of  $\sim 50\%$ . The crack length was measured by an optical microscope under a magnification of 500 by stopping the test and removing the speci-

men from the machine. The difference in crack length on the two surfaces of the specimen was less than 10%. This difference remained unchanged during the crack propagation and the average crack length was quoted to calculate the stress intensity factor.

Tests began at an applied maximum cyclic load of 300 N. Load was increased by 10 N every  $10^5$  cycles until a fatigue pre-crack was initiated from a straight-through notch. Cracks were always found to decelerate first and to be arrested finally with the number of cycles. The load was then increased by 10 N to restart the crack until the crack length increased steadily with the number of cycles at a certain load amplitude. Crack growth rates were controlled under load-decreasing conditions to approach to the fatigue threshold stress intensity range,  $\Delta K_{\text{th}}$ . The value of  $\Delta K_{\text{th}}$ , below which long cracks are presumed to be dormant, was operationally defined at a maximum growth rate of  $10^{-10}$  m/cycle. After finishing threshold measurements the load amplitude was kept constant until the specimens failed. An experiment at constant  $K_{\max}$  with decreasing- $K_{\min}$  ( $R$  is variable) was performed in order to elucidate the contribution of  $\Delta K$  and  $K_{\max}$  to the crack growth rate and corresponding mechanisms.

## 3. Results and discussion

### 3.1. Small crack behavior

Cyclic fatigue crack length versus number of cycles at different load amplitudes after pre-

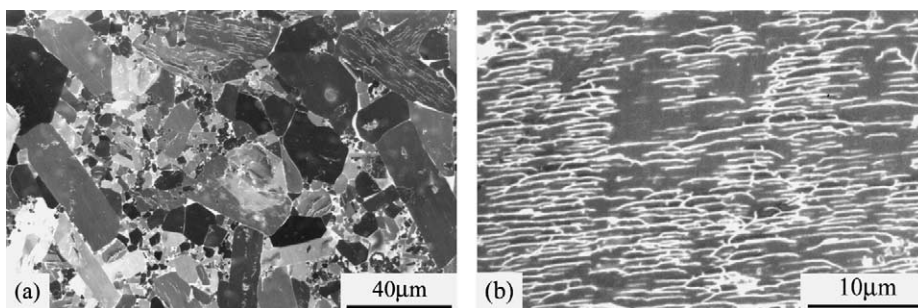


Fig. 1. Optical micrographs of pulse discharge sintered  $\text{Ti}_3\text{SiC}_2$ . (a) Microstructure after etching, (b) layered nature in an elongated grain.

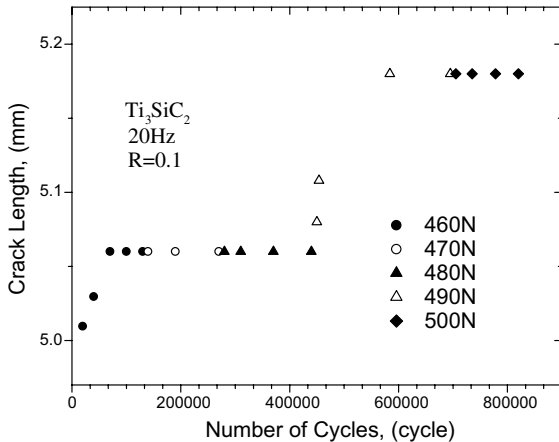


Fig. 2. Cyclic fatigue crack length,  $a$ , is plotted as a function of number of cycles at a load ratio  $R$  of 0.1 in  $\text{Ti}_3\text{SiC}_2$  at a relatively shorter crack length. The maximum applied loads are indicated in the figure.

cracking is shown in Fig. 2. Cracks were often observed to propagate and arrest completely during the first applied  $\sim 10^5$  cycles until a higher load amplitude is applied. This behavior is presumably caused by a faster increase in crack resistance as compared to the increase in driving force for crack growth based on the applied stress intensity. Such a phenomenon is often observed in the small crack region in the fatigue of metals and this may be regarded as “small crack” behavior. This is presumably caused by the principal role of crack bridging by single or clusters of grain in the wake of crack tip. Such bridging zone may produce shielding stress intensity,  $K_{sh}$ . It is assumed that the applied stress intensity,  $K_{appl}$  must exceed the sum of the intrinsic toughness,  $K_0$ , and  $K_{sh}$ , i.e.:

$$K_{appl} \geq K_0 + K_{sh}$$

in order for a crack to propagate. Here  $K_{sh}$  generally increases during crack propagation if the shielding bridging zone is not fully evolved. Therefore it is presumed that the shielding stress intensity,  $K_{sh}$ , increase with the crack length faster than the applied stress intensity,  $K_{appl}$ , and this results in a decrease in stress intensity experienced at the crack tip, and therefore in a reduced crack growth rate. When a certain crack length is exceeded,  $K_{appl}$  increases faster than  $K_{sh}$  and, thence,

crack length may begin to increase monotonically with the applied stress intensity.

### 3.2. Cyclic fatigue crack growth rate behavior

The contribution of cyclic and static fatigue to crack growth rate in  $\text{Ti}_3\text{SiC}_2$  is shown in Fig. 3. The maximum load remained the same of 525 N in the two loading modes, i.e. cyclic fatigue and static fatigue. The experimental results indicated that crack growth rates under cyclic fatigue were significantly faster than that under static fatigue. The cracks can be arrested under static loading, implying that the contribution to the crack growth from static loading could be ignored compared to that from cyclic loading.

Cyclic fatigue crack growth rates,  $da/dN$ , plotted as functions of the applied stress intensity range,  $\Delta K$ , and the maximum applied stress intensity,  $K_{max}$ , is shown in Fig. 4. It can be seen that  $\text{Ti}_3\text{SiC}_2$  is more sensitive to the applied driving force than ductile metals or bulk amorphous alloys. A marked dependence of crack growth rate on load ratio  $R$  is also observed in Fig. 4a, where crack growth rates are accelerated and the thresholds  $\Delta K_{th}$  reduced with increasing  $R$  at a fixed  $\Delta K$ . Whereas, in Fig. 4b, the influence of  $R$  on the crack growth rate is obscure and the slope of crack growth rate decreased slightly with increasing  $R$ . These behaviors of high exponents  $m$  and

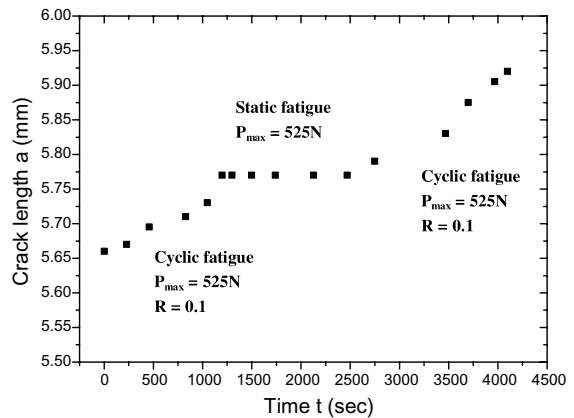


Fig. 3. Crack length,  $a$ , is plotted as a function of time,  $t$ , showing the contribution of cyclic and static fatigue to crack growth rate in  $\text{Ti}_3\text{SiC}_2$ .

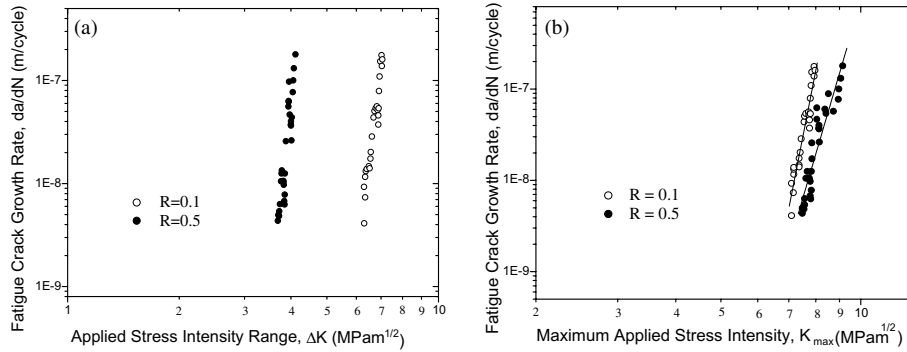


Fig. 4. Relationship between crack growth rates,  $da/dN$ , and (a) the applied stress intensity range,  $\Delta K$ , (b) the maximum applied stress intensity,  $K_{max}$ , for  $Ti_3SiC_2$  at load ratios,  $R$ , of 0.1 and 0.5.

dependence of crack growth rate on  $R$  have been observed in the fatigue crack growth of many typical ceramic materials, such as alumina [10], silicon nitride [11], yttria-stabilized zirconia [12], in situ toughened silicon carbide [13] and fine-grained alumina [14]. These behaviors indicate a strong dependence of the crack growth rate on  $K_{max}$  and weak dependence on  $\Delta K$ .

In order to discern the contribution to crack growth rates from  $\Delta K$  and  $K_{max}$ , a modified Paris power-law relationship

$$da/dN = C'(K_{max})^n(\Delta K)^p \quad (1)$$

is used which is often utilized to elucidate the fatigue mechanism of some structural ceramics. Here  $C'$ ,  $n$  and  $p$  are experimentally determined parameters.

Eq. (1) can be written in the more traditional form of the Paris power-law expression of the form [15]:

$$da/dN = C(\Delta K)^m \quad (2)$$

by using  $K_{max} = \Delta K/(1 - R)$ .

From Eqs. (1) and (2) the following relationship is obtained:

$$n + p = m$$

$$C' = C(1 - R)^n$$

For a fixed  $K_{max}$ , Eq. (1) becomes:

$$da/dN = D(\Delta K)^p,$$

$$\text{here } D = C'(K_{max})^n.$$

When the crack growth rate is plotted as a function of the applied stress intensity range,  $\Delta K$ , at a constant  $K_{max}$ , a much more stable crack propagation is observed. Fig. 5 shows the relationship between the crack growth rate,  $da/dN$ , and the applied stress intensity range,  $\Delta K$ , at a constant  $K_{max}$  ( $= 7.83 \text{ MPa m}^{1/2}$ ). The exponent  $p$  from the slope of double-logarithmic plot of  $da/dN$  versus  $\Delta K$  in this figure is 3.4. Therefore, we can see that  $n$  is equal to 22.6 when taking the exponent  $m$  of 26 at  $R = 0.1$  in Eq. (2). It is presumed that the exponent  $p$  obtained in Fig. 5 decreases at higher  $K_{max}$ , for the  $K$ -dependence of growth rates decreases as  $K_{max}$  approaches  $K_c$ .

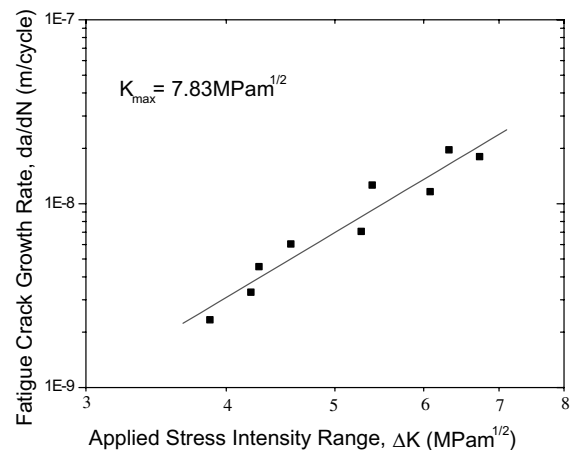


Fig. 5. Fatigue crack growth rate,  $da/dN$ , is plotted as a function of the applied stress intensity range,  $\Delta K$ , at a constant  $K_{max} = 7.83 \text{ MPa m}^{1/2}$  in  $Ti_3SiC_2$ .

As compared to  $\Delta K$ , the experimental results demonstrate clearly a strong dependence of crack growth rates on  $K_{\max}$ . Similar to many typical ceramics, these observations on cyclic fatigue of  $\text{Ti}_3\text{SiC}_2$  disclosed a fatigue mechanism controlled predominantly by  $K_{\max}$  at the crack tip and weakly by shielding through ligaments or grain bridging in the wake of crack tip. In comparison with typical ceramic materials, the crack growth rate in  $\text{Ti}_3\text{SiC}_2$  exhibits slightly higher dependence on the stress intensity factor range. Such a relatively stronger dependence can be seen from the significant change of slopes of crack growth rates from 15.1 to 25.9 in Fig. 4b when  $R$  changes from 0.5 to 0.1. This result suggests a strong mechanical damage to the bridging under cyclic loading. Such strong mechanical damage presumably originates from the existence of profuse grains bridging sites on the crack surfaces in the wake of crack tip.

### 3.3. Fatigue crack path observations

Compared to many typical ceramics,  $\text{Ti}_3\text{SiC}_2$  exhibits lower crack growth rates and higher threshold stress intensity factor. This behavior originates from its microstructural characteristics, i.e. structural heterogeneity with elongated plate-like grains and layered nature of grains with delamination along basal plane. A clear intergranular fracture mode and intact grain bridging in the wake of crack tip can be clearly seen from the crack path in the region of cyclic fatigue, as shown in Fig. 6a. Occasionally, a crack may propagate along the grain boundary at a right angle to its original direction. Besides, basal plane slipping traces in isolated grains along the crack path is frequently observed, indicating an additional energy dissipation due to friction. In addition, extensive crack deflection and branching, which are

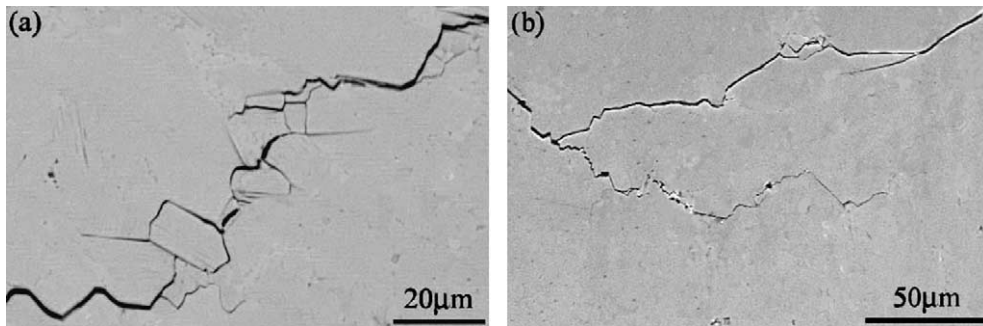


Fig. 6. Scanning electron micrographs of the crack path morphology showing (a) the predominantly intergranular fracture and profuse intact grain bridging. (b) cracks deflection and branching. The crack propagation direction is from left to right.

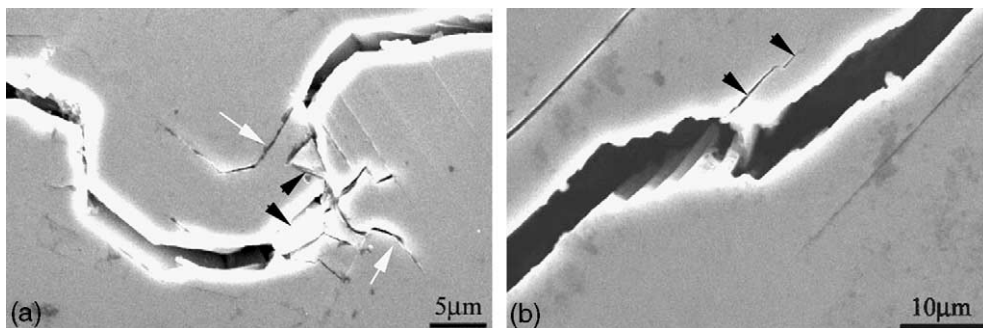


Fig. 7. Scanning electron micrographs of (a) branching crack (indicated by white arrows) and wear debris (indicated by black arrows) caused by strong frictional traction and wear between grains, (b) basal plane slipping traces (indicated by arrows) and formation of microfaults in grains of  $\text{Ti}_3\text{SiC}_2$  in the wake of crack tip. The crack propagation direction is from left to right.

characteristic features of high-toughness structural ceramics, can be seen in Fig. 6b.

As shown in Fig. 7a, branching cracks and wear debris can be observed in the wake of crack tip indicative of considerable local frictional traction of bridging grains. Besides, shear-induced micro-faults are clearly observed in an individual grain, as shown in Fig. 7b, which can reduce the frictional pullout stress at the grain/matrix interface under cyclic fatigue. All these observations reflect the operation of multiple energy dissipative mechanisms, which render  $\text{Ti}_3\text{SiC}_2$  to exhibit a higher threshold stress intensity and a lower crack growth rate.

The heterogeneous and laminated structure suggests some special toughening mechanisms, i.e., multi-lamellae slip along basal planes and micro-cracking in the weak grain boundary which promote bridge formation. Similar deformation characteristics have also been found in mica-containing glass-ceramics with a heterogeneous grain structure [16]. Such microstructure and deformation modes have been shown to be susceptible to damage accumulation during cyclic fatigue by providing easy fracture paths along weak interfaces. In  $\text{Ti}_3\text{SiC}_2$ , this damage by cyclic fatigue has been demonstrated by profuse wear debris and a distinct increase in slope of crack growth rate with decreasing  $R$  in the plot of  $da/dN$  versus  $K_{\max}$ .

#### 4. Conclusions

$\text{Ti}_3\text{SiC}_2$  exhibits a cyclic fatigue crack propagation behavior similar to typical structural ceramics, i.e. a much larger dependence of crack growth rates on  $K_{\max}$  as compared to  $\Delta K$ . However, a relatively higher threshold stress intensity and lower crack growth rate reflect its higher fatigue resistance. At a relatively short crack length, crack growth rates are often seen to decrease with the number of cycles, reflecting a faster increasing

in crack growth resistance through grain bridging than the applied crack driving force. The high fatigue resistance originates from the heterogeneous and laminated structure typical of  $\text{Ti}_3\text{SiC}_2$ . Such microstructure may lead to extensive energy dissipation through microfaults, crack deflection, branching and intact grain bridging.

#### Acknowledgement

This work was subsidized with the Special Funds for the major State Basic Research Projects under No. 19990650.

#### References

- [1] Barsoum MW, EI-Raghy T. *J Am Ceram Soc* 1996;79:1953.
- [2] Low M, Lee SK, Lawn BR. *J Am Ceram Soc* 1998;81:225.
- [3] EI-Raghy T, Zavaliangos A, Barsoum MW, Kalidindi SR. *J Am Ceram Soc* 1997;80:513.
- [4] Low M. *J Eur Ceram Soc* 1998;18:709.
- [5] Zhang ZF, Sun ZM, Hashimoto H, Abe T. *Acta Mater*, submitted for publication.
- [6] Gilbert CJ, Bloyer DR, Barsoum MW, Tomsia AP, Ritchie RO. *Scripta Mater* 2000;42:761.
- [7] Barsoum MW, EI-Raghy T. *Metall Mater Trans* 1999;30A:363.
- [8] Barsoum MW, Farber L, EI-Raghy T. *Metall Mater Trans* 1999;30A:1727.
- [9] Radovic M, Barsoum MW, EI-Raghy T, Wiederhorn SM, Luecke WE. *Acta Mater* 2002;50:1297.
- [10] Reece MJ, Guiu F, Sammur FR. *J Am Ceram Soc* 1989;72:348.
- [11] Jacobs DS, Chen I-W. *J Am Ceram Soc* 1995;78:513.
- [12] Liu S-Y, Chen I-W. *J Am Ceram Soc* 1991;74:1206.
- [13] Gilbert CJ, Cao JJ, Moberlychan WJ, Dejonghe LC, Ritchie RO. *Acta Mater* 1996;44:3199.
- [14] Gilbert CJ, Ritchie RO. *Fatigue Fract Eng Mater Struct* 1997;20:1453.
- [15] Paris PC, Erdogan F. *J Bas Eng Trans ASME* 1963;85:528.
- [16] Cai H, Kalceff MAS, Hooks BM, Lawn BR, Chyung K. *J Mater Res* 1994;9:2654.